Effects of Nonequilibrium and Wall Catalysis on Shuttle Heat Transfer

C. D. Scott
NASA Johnson Space Center, Houston, Texas

Nomenclature

ALT = altitude
C = atom mass fraction
f = heat flux adjustment factor defined in Eq. (2)
h_D = enthalpy of formation of species
h_T = total enthalpy
k = Boltzmann constant
k_w = catalytic recombination rate
L = length of vehicle
m = mass of atom
P = pressure
R_n = nose radius
q = heat flux
S = surface distance
T = temperature
t = time from entry interface ($Z = 122$ km)
V = velocity
V_{INF} = freestream velocity
X = axial distance from nose
y = distance from body
Z = geometric altitude
α = angle of attack
γ = energy-transfer catalytic combination coefficient
ϵ = emittance
ρ = density
σ = Stefan-Boltzmann constant

Subscripts

FC = fully catalytic
N = nitrogen
NC = non-catalytic
O = oxygen
ref = reference condition or property
ω = wall
∞ = freestream

Introduction

THE Shuttle Orbiter is a hypersonic glide re-entry vehicle that spends much of its entry time at relatively tenuous altitudes in which chemical nonequilibrium predominates in the shock layer. Calculations have shown that both dissociation nonequilibrium[1,2] and recombination nonequilibrium exist.[1] On the windward side, the dissociation nonequilibrium exists in the inviscid layer and the recombination nonequilibrium exists in the boundary layer. It is also expected that nonequilibrium exists in the leeside flow, but theoretical predictions are virtually nonexistent. However, there is some experimental substantiation discussed here. Verification of nonequilibrium phenomena has not been directly obtained via species concentration measurements; however, these phenomena are inferred by comparing heat-transfer measurements with the reacting flowfield results.

Although measurements of surface temperatures on the high-temperature reusable surface insulation (HRSI) tiles have been made at numerous locations of the Orbiter, this paper primarily addresses measurements on or near the windward centerline of the lower fuselage because predictions of local flow conditions are much easier to obtain in this region. The presence of chemical nonequilibrium was made easier to verify because the HRSI tile reaction-cured glass (RCG) coating is relatively noncatalytic with respect to atom recombination and dissociation energy accommodation. Also of great importance in demonstrating the nonequilibrium flow behavior is the catalytic surface effects experiment performed on several orbiter flights by Stewart, Rakich, and Lanfranco,[3,4] the initial results of which were reported in Ref. 5. Prior to the flight experiments, predictions of the noncatalytic nature were reported in Refs. 1-3 based on flowfield computations and arcjet experiments. Besides the results reported in Ref. 5, other calculations have been made for the RCG-coated tiles and compared with flight measurements. Scott and Derry[6] used the reacting flowfield/boundary-layer method of Ref. 2 with measured energy-transfer catalytic recombination coefficients of Ref. 7 and compared those predictions with flight measurements. Likewise, Shinn, Moss, and Simmonds[8] computed heat fluxes using an axisymmetric reacting viscous shock-layer code with the recombination coefficients of Ref. 7 and showed better agreement with flight measurements. Recently, Kim, Swaminathan, and Lewis[9,10] solved the three-dimensional shock-layer equations for the Shuttle geometry and obtained encouraging results.

Another method briefly discussed here is that of Harthun, Blumer, and Miller,[11] who computed the equilibrium heat flux by a wind tunnel data correlation and then corrected it for nonequilibrium effects using a catalytic heating parameter inferred from the flight measurements. Unfortunately, the documentation of their method in the available literature is incomplete.

This paper reviews the recent applications of nonequilibrium flowfield computations or methods as they apply

---

Carl D. Scott received his B. A. degree in physics from Rice University in 1960 and his Ph.D. degree in physics from the University of Texas in Austin in 1969. He joined NASA's Johnson Space Center (JSC) in 1963 after service in the Navy. In his early years at JSC, he studied arcjet plasma and flow diagnostics and did his Ph.D dissertation on spectral line broadening of helium in arcjet flows. As research engineer, he has done experimental and theoretical work in the aerothermodynamic areas of catalytic atom recombination, reacting flowfields, and associated convective heating. Most of this work was directed toward the Space Shuttle effort. Dr. Scott is an Associate Fellow of AIAA and a member of the AIAA Thermophysics Technical Committee.

Presented as Paper 83-1485 at the AIAA 18th Thermophysics Conference, Montreal, Canada, June 1-3, 1983, received March 9, 1984, revision submitted Oct. 3, 1984.

to the Space Shuttle Orbiter re-entry. Much research has preceded and contributed to the development of these techniques; however, for details on their development, one should consult the references in the principal papers cited here. To list all prior contributions would dilute the focus of this paper.

This paper critically evaluates the various flowfield predictions in the nonslip flow regime, comparing the results of equilibrium and nonequilibrium flowfields coupled with reacting axisymmetric analog boundary-layer solutions and the results of viscous shock-layer solutions with flight temperature/heat flux measurements near the windward centerline for the Shuttle flights STS-2, STS-3, and STS-5. Recombination coefficients inferred from arcjet and flight results are also compared.

In the comparisons with flight heat flux measurements, there is concern with two basic aspects of the predictions: the flowfield methodology and the surface catalytic recombination phenomena. The first aspect can be subdivided into dynamical and geometrical characteristics, thermophysical properties, and gas-phase chemical reaction kinetics. The second aspect can be subdivided into wall recombination rates of the basic thermal protection material, contamination issues, and knowledge gained from the catalytic surface effects experiment. All of these aspects are interrelated and the Shuttle flights do not provide an experiment in which each aspect can be controlled independently. Numerical simulation is capable of single-parameter variation, but confirmation of the results is difficult because of flight complexities and unknowns. Particularly, there is no measurement of the chemical composition of the flow. The paper considers flowfield chemical composition effects (equilibrium vs nonequilibrium), methods of solution (two-layer and viscous shock-layer approaches), and surface catalytic recombination rates; and it touches on possible contamination on the surface. The issues of incomplete chemical energy accommodation of catalytically formed excited species and subsequent quenching are not explored.

Computational Methods and Their Application

Five computational methods based on flowfield computations are considered here. The methods are subdivided into applications and are further subdivided into particular cases, which are summarized in Table 1. The method of Harthun et al.[11] is briefly mentioned.

The first two methods are axisymmetric viscous shock-layer methods of Moss[12] and Miner and Lewis.[13] The next two are two-layer approaches. Rakich and Lanfranco[2] treated the three-dimensional reacting inviscid flowfield and used the results for reacting boundary-layer edge conditions. Goodrich et al.[14] solved the equilibrium three-dimensional inviscid case and used their results as edge conditions for equilibrium boundary-layer solutions. The fifth method is the three-dimensional nonequilibrium viscous shock-layer method of Kim, Swaminathan, and Lewis.[9,10]

Shinn, Moss, and Simmonds[8] applied the Moss method[12] with variable wall recombination coefficients to the Shuttle Orbiter by approximating the Shuttle geometry with hyperboloids of revolution fitted by Zoby.[15] They presented cases for various times in the Orbiter entry and concluded that: *the Shuttle flight data indicate the shock-layer flow is appreciably in nonequilibrium down to an altitude of 50 km.* Scott's extrapolated recombination rates used in their viscous shock-layer calculations result in good agreement with flight data forward, but not aft, on the vehicle. Better agreement aft is obtained if $k_{wO} = 100$ cm/s is used. The temperature of the surface during entry is 80-200 K less than were the surface fully catalytic.

Gupta et al.[16] similarly applied the Moss method[12] with various recombination coefficients and for a range of Orbiter angles of attack. They found that a ± 5 deg variation in angle of attack does not affect the nonequilibrium heating appreciably at 75 and 48 km altitudes. The temperature dependence of the oxygen recombination rate is not as steep as an extrapolation of Scott's data[7] indicates. They concluded that a value of $k_{wO} = 200$ cm/s seems to yield better agreement with the flight measurement of heat flux at certain locations and flight regimes. A 49% reduction in heating due to nonequilibrium effects was noted in the nose regions at $X/L = 0.025$ and 75 km altitude. Nonequilibrium effects on the heating are not significant below about 65 km even though the flow may not be in equilibrium, indicating that

Table 1 Methods and applications presented in plots

Application No.	Method, Ref. No.	Application, Ref. No.	Wall boundary condition	Flowfield	Boundary layer	
					Edge condition	Chemistry
1	12	8	Ref. 7	VSL[a] nonequilib.	N/A[b]	N/A
2	12	8	ECW[c]	VSL nonequilib.	N/A	N/A
3	12	8	Noncata.	VSL nonequilib.	N/A	N/A
4	12	8	Equilib.	VSL equilib.	N/A	N/A
5	13	Present	Ref. 7	VSL reacting	N/A	N/A
6	13	Present	Fully cata.	VSL reacting	N/A	N/A
7	13	Present	Noncata.	VSL reacting	N/A	N/A
8	14	14	Equilib.	3D inviscid equilib.	Equilib.	Equilib.
9	2	Present	Fully cata.	3-D inviscid nonequilib.	Nonequilib.	Nonequilib.
10	2	Present	Ref. 7	3D inviscid nonequilib.	Nonequilib.	Nonequilib.
11	2	Present	Noncata.	3D inviscid nonequilib.	Nonequilib.	Nonequilib.
12	14	Present	Fully cata.	3D inviscid equilib.	Equilib.	Nonequilib.
13	14	Present	Noncata.	3D inviscid equilib	Equilib.	Nonequilib.
14	2	Present	Ref. 5	3D inviscid nonequilib.	Nonequilib.	Nonequilib.
15	10	10	Noncata.	3D VSL nonequilib	N/A	N/A

[a]VSL = Viscous shock layer. [b]N/A = Not applicable. [c]ECW = Equilibrium catalytic wall.

equilibrium boundary-layer methods or heating correlations of the type suggested by Rakich et al.[5] may be useful

The method of Rakich and Lanfranco[2] was applied by Rakich et al.[5] to calibrate an approximate method that uses equilibrium normal shock isentropic boundary-layer edge conditions in lieu of the reacting variable-entropy edge conditions. This approximate method was then used to infer k_{wO} of the RCG-coated HRSI tiles and to infer k_{wO} of the iron-cobalt-chromia spinel (C742) coating used in the catalytic surface effects flight experiment tiles. They inferred that $k_{wO} = 80$ cm/s and *assumed* that $k_{wN} = 0.3\, k_{wO}$ for RCG at T_w of about 1100 K. In their later paper, Stewart et al.[4] obtained a temperature-dependent (Arrhenius) relation for k_{wO} using the comparison of flight measurements with an approximate analysis. Their catalytic surface effects experiment demonstrated that the flow is indeed in chemical nonequilibrium.

Rakich's method[2] was also used by Scott[6] with temperature-dependent recombination coefficients inferred from arcjet measurments.[7,17] He used the reacting boundary-layer code BLIMPK developed by Bartlett and Kendall[18] and extended by Tong, Buckingham, and Morse.[19] This method resulted in higher heating than measured on the nose of the Orbiter, but tended to predict or underpredict the heating on the midbody. These results are presented here for comparison with other results.

Reacting boundary-layer calculations were made with equilibrium edge conditions provided by Goodrich et al.[14] along with different wall recombination assumptions. These results are presented here. Miner and Lewis' axisymmetric, reacting viscous shock-layer code[13] was applied with various catalytic wall assumptions and those results are likewise presented here.

The fifth computational method considered herein for nonequilibrium flow calculations applied to the Space Shuttle was presented by Kim, Swaminathan, and Lewis.[9,10] Those recent papers addressed the windward side of the Space Shuttle, applying the three-dimensional nonequilibrium shock-layer method with noncatalytic boundary conditions. Their windward centerline results for two points in the STS-2 trajectory are presented here.

Measurements of Heat Flux to Shuttle

Surface temperature measurements of several instrumented HRSI tiles, distributed along the lower surface of the Orbiter, are considered in this paper. The flights considered are STS-2, STS-3, and, to a limited extent, STS-5. Trajectory information was obtained from acceleration measurements on the Orbiter and from atmosphere models calibrated by atmospheric soundings. The resulting best estimated trajectories (BET) were obtained from the Mission Planning and Analysis Division at the NASA Lyndon B. Johnson Space Center. Heat fluxes were inferred from the measured temperatures by computing the corrected radiation equiibrium heat flux.

$$q = 1.06\epsilon\sigma T_w^4 f \tag{1}$$

The factor 1.06 accounts for the fact that the thermocouples lie about 0.38 mm beneath the surface coating and for conduction in the tile. This factor was obtained from the method of Williams and Curry,[20] who inferred heat fluxes from temperatures using an inverse thermal math model formulation.† Over the range of time in the trajectory and temperatures considered in this paper, a correction factor of 1.06 is accurate to within 2-3%.

When comparing the measurements of one flight with another or when comparing calculations with measurements, it is necessary to adjust the heat fluxes to account for differences in the freestream conditions. Since the hypersonic stagnation point heating is approximately proportional to $\rho_\infty^{1/2} V_\infty^3$, all points are corrected by the ratio of that factor for the two freestream conditions, i.e.,

$$f = (\rho_\infty / \rho_{\infty \mathrm{ref}})^{1/2}\ (V_\infty / V_{\infty \mathrm{ref}})^3 \tag{2}$$

The flight heating rates are used as reference conditions when flight measurements are compared with calculations. The heat fluxes are then presented in absolute units as obtained from Eq. (1). The factor f is probably accurate to within $\pm 3\%$ as verified by a comparison of calculations using the Miner and Lewis code.[13] All the comparisons were made for an angle of attack of about 40 deg.

To determine the consistency from flight to flight, the bottom centerline heat flux measurements for STS-2, STS-3, and STS-5 are compared at three different times in the flights as shown in Figs. 1-3, respectively. The corresponding freestream conditions are given in Table 2. It is seen that the flight-to-flight repeatability is about 15-30% and the standard deviation about the mean at each X/L is about $\pm 10\%$. The STS-2 heat fluxes are consistently lower than those of the other two flights at almost all locations. The reason for this difference is not understood, but it may be related to a change in catalycity resulting possibly from contamination of the surface or to a change in emittance. The heat rate correction for these cases is no larger than 7%, as seen in Table 2. The measurment at $X/L = 0.695$ seems anomalously low and, therefore, may be a bad measurement. The rather large discrepancy in the measurement for STS-2 compared with the other two flights at $X/L = 0.14$ also is not understood.

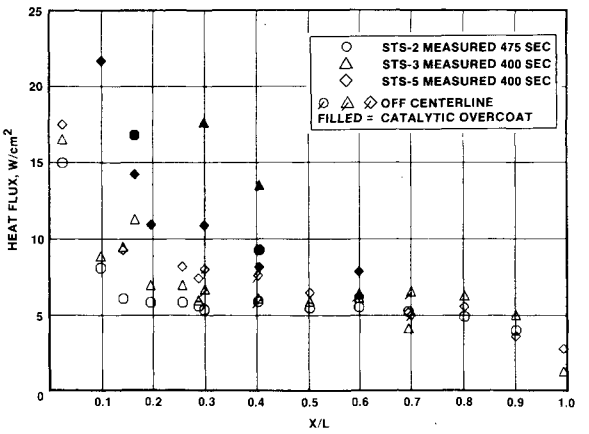

Fig. 1 Measured radiation equilibrium heat fluxes near windward centerline of Orbiter (reference STS-2: $V_{INF} = 7.16$ km/s, ALT = 74.7 km).

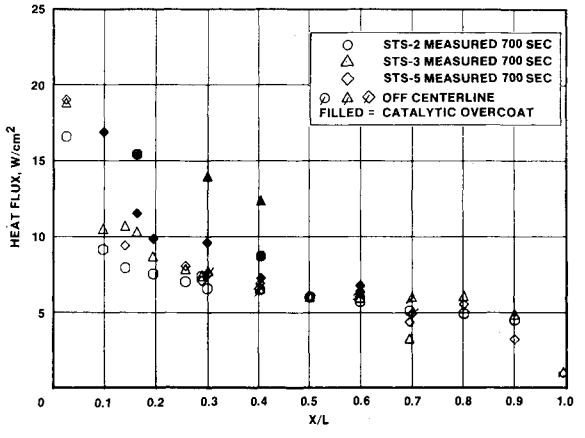

Fig. 2 Measured radiation equilibrium heat fluxes near windward centerline of Orbiter (reference STS-2: $V_{INF} = 6.57$ km/s, ALT = 70.2 km).

†The author is grateful to S. D. Williams of Lockheed Engineering and Management Services Co. for calculating the heat flux for this determination.

Shuttle Centerline Pressures

Pressure measurements during the time of high heating on the Orbiter were obtained only during STS-3 and STS-5. These measurements, normalized by $\rho_\infty V_\infty^2$ are presented in Fig. 4 along with values calculated by four methods. It is seen that the flight-to-flight repeatability is very good at almost all locations. The pressure decreases very rapidly in the forward 10% of the vehicle, then remains almost constant from X/L of 0.1-0.4, rising slightly to $X/L=0.8$. The three-dimensional flowfield calculations of Rakich and Lanfranco[2] and Goodrich et al.[14] agree with the measurements within about 5%, except in the vicinity of $X/L=0.1$ where the calculations are about 20% higher than the measurments. The calculations using the Miner and Lewis code[13] agree within about 10%, except at $X/L=0.1$ where the agreement is within about 12%. Also shown is the pressure predicted by Kim et al.,[9] where it is seen that the predicted pressure is 10-20% lower than those measured aft of $X/L=0.2$. Their agreement is best on the forward part on the vehicle, but differs most significantly at $X/L>0.7$. The large discrepancy in the other methods at $X/L=0.1$ may result from an experimental error due to a negative bias of unknown amount.[21] The instrumentation and signal processing of the pressure measurements result in only positive readings. The existence of a negative bias was indicated by a measurement that did not exceed zero until a time later than expected for the flight condition. (See Ref. 21.) If the error associated with the negative bias is small, then the calculations appear in error at $X/L=0.1$. Although a direct comparison of the geometries has not been made, it is possible that the geometry descriptions in the flowfield codes do not adequately describe the vehicle as actually built; otherwise, these codes do not adequately handle the rapid expansion around the nose, overpredicting the pressure (and heat flux) near $X/L=0.1$

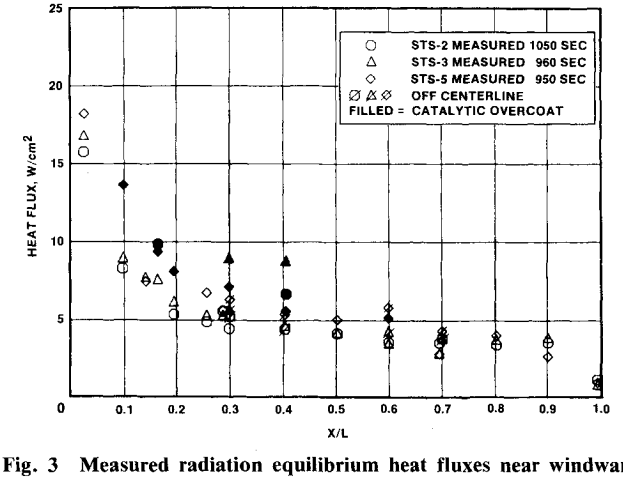

Fig. 3 Measured radiation equilibrium heat fluxes near windward centerline of Orbiter (reference STS-2: $V_{INF}=4.56$ km/s, ALT = 57.2 km).

Heat Flux Comparisons

In the following comparisons, the author has used the results of others and, in some cases, the author—not the developers of the methods—is responsible for any error or misapplication of the method.

Equilibrium and Nonequilibrium: Two-Layer Methods and Viscous Shock Layer Methods

In the past, it has been shown that the heat flux predicted by equilibrium calculations and by reacting calculations with a fully catalytic wall are approximately equal. To verify this for the two boundary-layer methods considered here, comparisons are made between the equilibrium results of Goodrich et al.[14] and those obtained using the Rakich and Lanfranco method.[2] The freestream conditions are given in Table 3. In Fig. 5, the Goodrich equilibrium prediction is compared with two nonequilibrium boundary-layer cases with fully catalytic walls. (Fully catalytic here means $\gamma_O=\gamma_N=1$, vis-a-vis $k_w=\infty$ or $C_{Ow}=C_{Nw}=0$.) The edge conditions in the last two cases are Goodrich equilibrium and Rakich and Lanfranco nonequilibrium. Given the same edge conditions, it is seen that the equilibrium boundary-layer calculation over the entire length of the vehicle is about 15% lower than the all-nonequilibrium calculation over the entire length of the vehicle. Evidently, the transport of chemical energy by diffusion is more efficient in this case than via conversion of chemical energy to thermal energy, which is then transported to the wall via conduction. The opposite result was obtained by Shinn et al.,[8] who found the equilibrium viscous shock layer resulted in

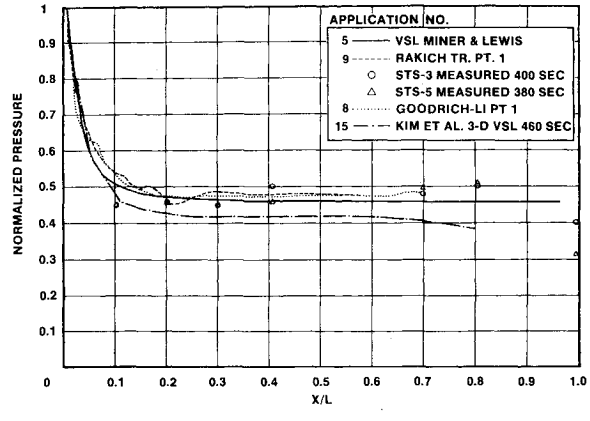

Fig. 4 Measured and calculated pressures on centerline of Orbiter, $t=460$ s ($V_{INF}=7.2$ km/s, ALT = 74.9 km).

Table 2 Freestream conditions[a] for corresponding heat flux measurements

Flight	Time,[b] s	V_∞, km/s	ρ_∞, kg/m³	α, deg	f[c]	Z, km	h_T, MJ/kg	$\rho_\infty V_\infty^2$ kPa
STS-2	475	7.16	0.412×10^{-4}	40.37	1.000	74.7	25.6	2.11
	700	6.57	0.807×10^{-4}	39.99	1.000	70.2	21.6	3.49
	1050	4.56	0.402×10^{-4}	40.56	1.000	57.2	10.4	8.35
STS-3	400	7.29	0.394×10^{-4}	40.02	1.033	75.1	26.6	2.09
	700	6.29	0.113×10^{-3}	39.58	1.037	68.2	19.8	4.46
	960	4.58	0.417×10^{-3}	40.72	1.032	57.6	10.5	8.75
STS-5	400	7.17	0.397×10^{-4}	40.05	0.986	74.9	25.7	2.04
	700	6.19	0.998×10^{-4}	40.71	0.926	61.9	19.2	3.79
	950	4.56	0.411×10^{-3}	39.19	1.010	54.0	10.4	8.54

[a]Best estimated trajectory. [b]Time from entry interface ($Z=122$ km). [c]Factor used to adjust heat flux relative to STS-2 condition, based on stagnation point theory. Defined in Eq. (2).

higher heating than did the equilibrium catalytic wall nonequilibrium case.

The comparison of the reacting boundary layer with equilibrium edge conditions vs nonequilibrium edge conditions indicates that, on the nose, there is very little difference between the two cases, whereas, the nonequilibrium edge conditions on the midfuselage result in about 15% lower heating. The nonequilibrium edge case with a fully catalytic wall is very close to the all-equilibrium calculation aft of $X/L = 0.2$. The latter agreement does not stem from the flow approaching equilibrium downstream, because the equilibrium nitrogen atom concentration both at the edge and in the boundary layer is greater than the nonequilibrium concentration by a factor of about 1.3 in this case. Moreover, it was shown in Ref. 1 that the boundary layer is virtually frozen. This will be discussed further in a subsequent section.

A comparison of the axisymmetric reacting viscous shock-layer method of Miner and Lewis[13] and the reacting two-layer approach of Rakich and Lanfranco[2] is made in Fig. 6, where the nonequilibrium boundary-layer result for a fully catalytic wall lies above the viscous shock-layer results by about 20% on the nose. Agreement improves to within about 11% at $X/L = 0.55$. The effect of edge conditions is about 10% or less everywhere for a fully catalytic wall. The results for a noncatalytic wall are given in Fig. 7, where it is seen that the boundary-layer heat flux is about 30% greater than the viscous shock-layer heating on the nose, but improves to about 10% at $X/L = 0.55$. Agreement of the reacting viscous shock-layer results and the reacting boundary layer with equilibrium edge conditions is within about 10% everywhere along the body. The equilibrium edge condition results fall below the nonequilibrium results on the nose, but they are very close farther aft.

Attention is now turned to a comparison of the axisymmetric viscous shock-layer method of Moss[12] as applied by Shinn et al.[8] and the two-layer method of Rakich and Lanfranco[2] applied here for a lower velocity and altitude situation. It is seen in Fig. 8 that the axisymmetric nonequilibrium viscous shock layer with equilibrium catalytic wall (ECW) and the equilibrium viscous shock layer (VSL) agree quite well (within about 5%). They also agree quite well with the Goodrich equilibrium two-layer result.[14] It is seen that the fully catalytic nonequilibrium two-layer results are greater by about 10-20% which is the same as noted for case 1. For the noncatalytic case, the agreement between the axisymmetric VSL and the two-layer methods (Fig. 9) is worse since the two-layer results are about 20-40% higher than the axisymmetric viscous shock-layer results of Shinn et al.[8] and the present results using the Miner and Lewis code.[13] The latter results seem to indicate that heat transfer by atom diffusion is more

Table 3 Freestream conditions for calculations

Parameter	Case 1	Case 1	Case 2	Case 460[a]	Case 650[a]
Method	BL[b]	VSL	BL	VSL	VSL
Velocity, km/s	7.62	7.62	6.614	7.20	6.73
Altitude, km	75.0	75.0	68.9	75.0	71.3
Angle of attack, deg	41.4	41.4	40.2	40.0	39.4
Density, $kg/m^3 \times 10^{+5}$	3.795	3.974	9.28	3.81	6.83
Total enthalpy, MJ/kg	29.0	29.0	21.8	25.9	22.6
Temperature, K	197	197	221	198	205
Stagnation point pressure, kPa	2.20	2.31	4.10	1.98	3.09
Nose radius, m	0.814	1.342	0.814	1.276	1.253
Hyperboloid angle, deg[c]	—	42.2	—	40.75	40.20
Lewis No. in shock layer					
Present calculations	—	1.0	—	1.0	1.0
Ref. 11	—	1.4	—	1.4	1.4
Ref. 16	—	1.4	—	1.4	1.4

[a]These freestream conditions are the same as the one in Ref. 7 for STS-2 times corresponding to the case number and the same as cases 2 and 3, respectively, in Ref. 8. [b]BL = boundary layer. [c]Not applicable to three-dimensional VSL.

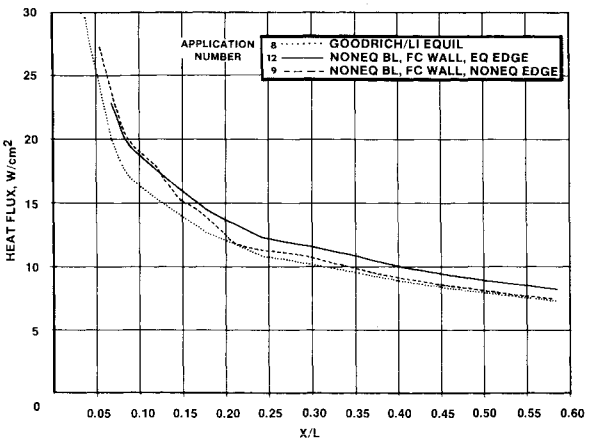

Fig. 5 Comparison of equilibrium and nonequilibrium boundary-layer calculations with fully catalytic wall, case 1 ($V_{INF} = 7.62$ km/s, ALT = 74.98 km).

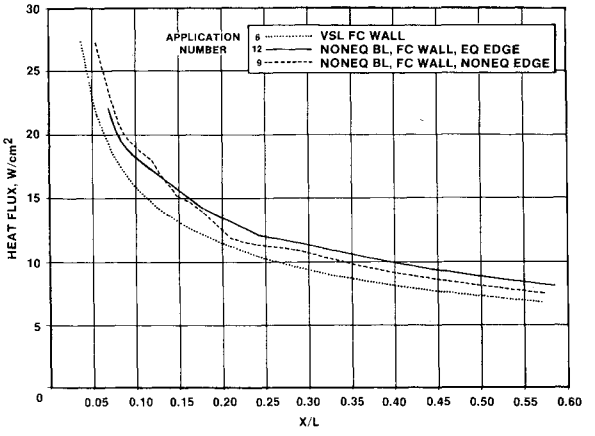

Fig. 6 Comparison of nonequilibrium axisymmetric viscous shock-layer and two-layer calculations with fully catalytic wall, case 1 ($V_{INF} = 7.62$ km/s, ALT = 74.98 km).

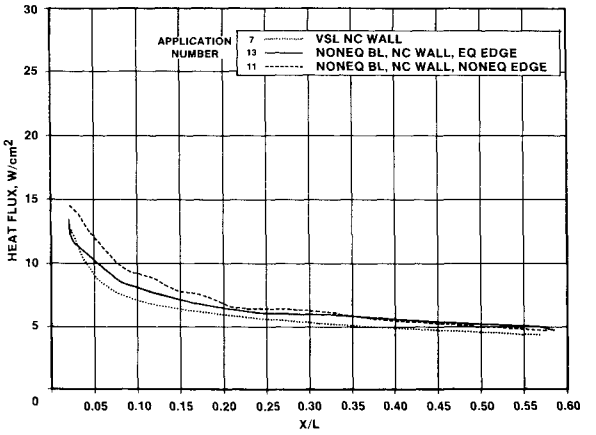

Fig. 7 Comparison of nonequilibrium axisymmetric viscous shock-layer with two-layer calculations having nonequilibrium and equilibrium edge conditions for noncatalytic wall, case 1 ($V_{INF} = 7.62$ km/s, ALT = 74.98 km).

important in the viscous shock-layer method. This hypothesis is consistent with the somewhat higher degree of dissociation, especially the nitrogen, associated with the viscous shock-layer calculation. The reason for the differences in the atom fraction in the two methods is not understood, since the reaction rates used in both methods were essentially the same. However, there may be differences in the shock shape that could lead to temperature profile and flow time differences and, thus, influence the degree of dissociation.

The recent three-dimensional nonequilibrium viscous shock-layer results[9] with a noncatalytic wall are also given in Fig. 9. The heat flux at $X/L<0.1$ is closer to the axisymmetric VSL results, but does not decrease as rapidly downstream. In fact, the three-dimensional heating results are higher than even the two-layer results aft of $X/L=0.2$ and 50% higher than the axisymmetric VSL results, even though the pressure is lower. (See Fig. 4.) The chemical reaction model[22] in all the methods is virtually the same. (Hoverever, ions are neglected in the Rakich and Lanfranco method.) Therefore, the differences seen are most likely due to differences in the computational method or the geometry of the body and shock layer.

Comparison of Measured and Calculated Heat Flux

Attention is now turned toward a comparison of the calculated heat flux and the measured values along the lower surface centerline. The comparison is at two times in each of two flights. The particular times were selected to match the velocity and the density as closely as practicable to the conditions used in the boundary-layer predictions for cases 460 and 650 in Table 3. It was not possible to match both velocity and density simultaneously. The resulting heat fluxes were adjusted for the mismatch by the factor f of Eq. (2). As mentioned earlier, the measured heat fluxes were inferred from the measured temperatures using Eq. (1), where $\epsilon=0.85$.

The surface catalytic reactions considered in all the techniques discussed here are:

$$N+N+\text{site}\rightarrow N_2+\text{site}$$
$$O+O+\text{site}\rightarrow O_2+\text{site}$$

The surface reactions involving NO are assumed to have a zero rate. This assumption would appear to have a negligible effect on the surface heat flux since the concentration of NO is much smaller than that of O and N. (See Ref. 23.)

Several choices of catalytic recombination coefficients were used, as well as boundary conditions for the two-layer and the axisymmetric shock-layer calculations. The energy-transfer catalytic recombination coefficients for nitrogen and oxygen recombination on the RCG tile coating are present in Figs. 10 and 11, respectively. The coefficients presented are those found in Refs. 4, 5, 7, and 11.‡ In those cases where a catalytic

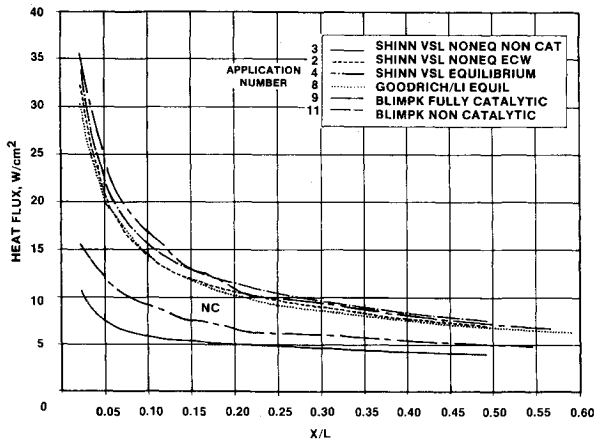

Fig. 8 Comparison of axisymmetric viscous shock-layer and two-layer calculations for STS-2 650 s case ($V_{INF}=6.73$ km/s, ALT = 71.29 km).

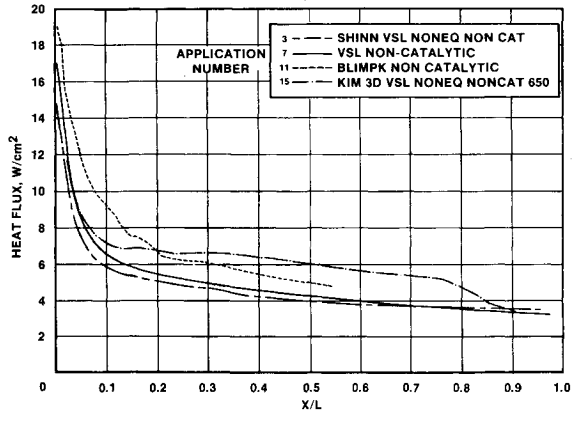

Fig. 9 Comparison of nonequilibrium axisymmetric and three-dimensional viscous shock-layer and two-layer calculations with noncatalytic wall for STS-2 650 s case ($V_{INF}=6.73$ km/s, ALT = 71.29 km).

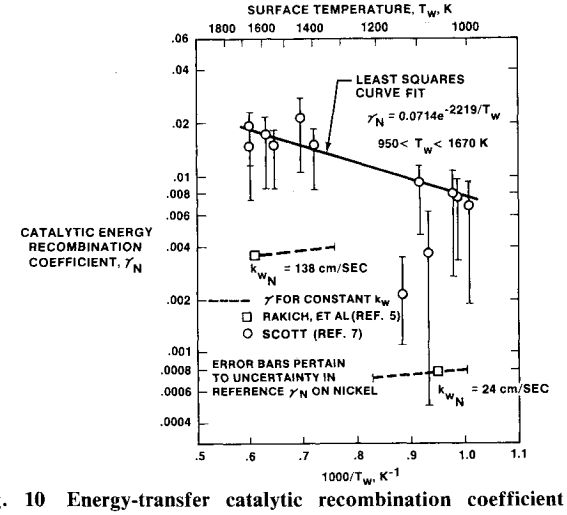

Fig. 10 Energy-transfer catalytic recombination coefficient for nitrogen on RCG-coated HRSI.

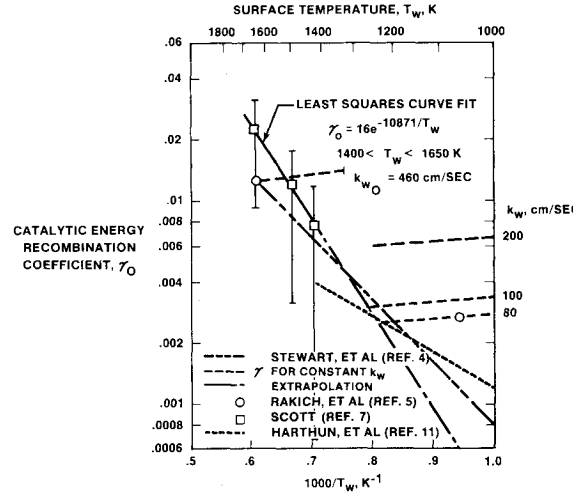

Fig. 11 Energy-transfer catalytic recombination coefficient for oxygen on RCG-coated HRSI.

‡There have been recent attempts to infer catalytic recombination rates from flight measurements. (See Refs. 23 and 24.) Although these attempts may be comforting if they lead to self-consistent results, they may also mislead one into accepting as accurate both an approximate calculational technique and the inferred recombination coefficients.

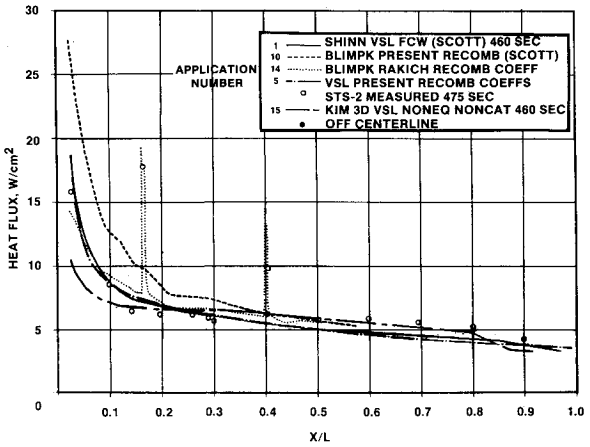

Fig. 12 Comparison of calculated and measured Shuttle heat fluxes for STS-2, $t = 475$ s ($V_{INF} = 7.16$ km/s, ALT = 74.7 km).

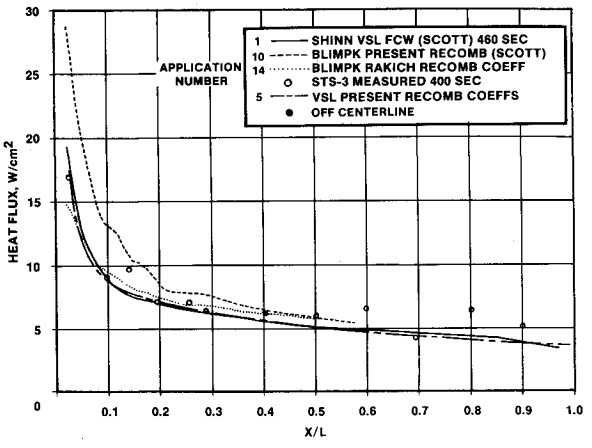

Fig. 14 Comparison of calculated and measured Shuttle heat fluxes for STS-3 $t = 400$ s ($V_{INF} = 7.29$ km/s, ALT = 75.1 km).

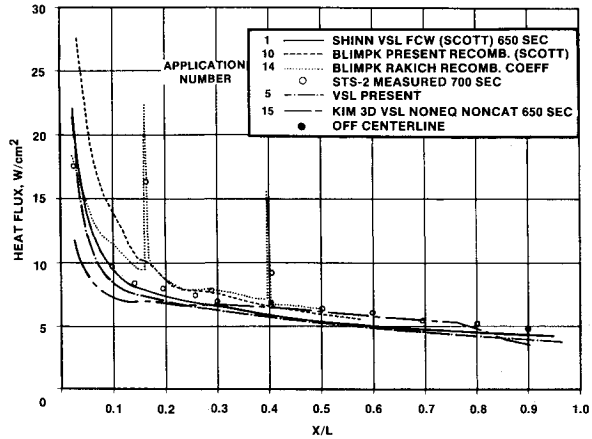

Fig. 13 Comparison of calculated and measured Shuttle heat fluxes for STS-2, $t = 650$ s ($V_{INF} = 6.73$ km/s, ALT = 71.29 km).

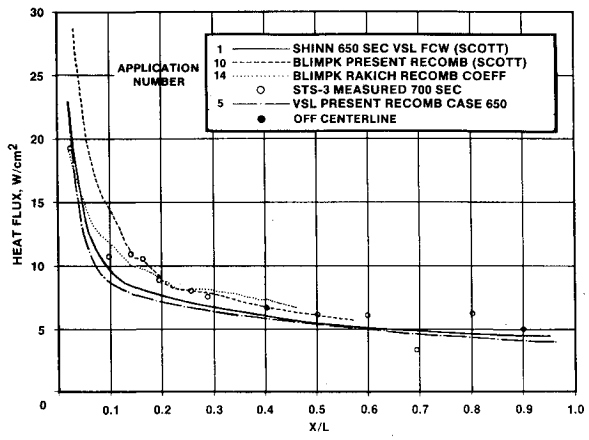

Fig. 15 Comparison of calculated and measured Shuttle heat fluxes for STS-3, $t = 700$ s ($V_{INF} = 6.29$ km/s, ALT = 68.21 km).

speed k_w was given, the recombination coefficient is plotted as a dashed line. The length indicates the temperature range over which k_w was used, where

$$\gamma = k_w \sqrt{2\pi m/kT}$$

It is seen in Fig. 10 that the inferred values of k_{wN} of Ref. 5 are 0.1-0.2 times the values of Ref. 7. This lack of agreement is not surprising since k_{wN} was *assumed* to be 0.3 times k_{wN} in Ref. 5. The values of γ_O (see Fig. 11) of Refs. 5 and 7 agree within experimental accuracy at the higher temperature range. At lower temperatures, $k_{wO} = 80$ cm/s is about a factor of 1.5-8 higher than the extrapolation of Ref. 7, depending on temperature. Extrapolating to such a low temperature can be inaccurate, but the extrapolation is generally consistent with other recombination measurements. (See Fig. 6 of Ref. 5.) Since the temperatures measured on the Shuttle fell mostly in the lower temperature range of 900-1100 K, the predictions of heat flux using the $k_{wO} = 80$ cm/s would result in higher heating, except on the nose or earlier in time where the nitrogen carries a larger part of the dissociation energy than oxygen.

Harthun, Blumer, and Miller[11] inferred from STS-2 flight measurements an effective temperature-dependent recombination coefficient. Their Arrhenius form does not discriminate between oxygen and nitrogen atom recombination. Their reference heat flux was based on fully catalytic predictions calibrated by wind tunnel measurements. Stewart, Rakich, and Lanfranco[4] also inferred the catalytic speed k_w from flight measurements using reference heat flux predictions based on reacting-boundary-layer solutions.[5] These two temperature-dependent Arrhenius functions are compared with oxygen recombination coefficents in Fig. 11 and are reasonably consistent with the oxygen recombination coefficients in Fig. 11 and are reasonably consistent with the oxygen arcjet results of Ref. 7, even though they represent a combination of oxygen and nitrogen recombination.

A comparison is made in Figs. 12-15 between the measurements and several calculations for STS-2 and STS-3 at two times in the trajectories. The measurements are near the bottom centerline of the vehicle except for a few points that are about 1.3 m off the centerline. In the higher altitude cases (Figs. 12 and 14), the viscous shock-layer methods with the temperature-dependent[7] γ_O and γ_N yield better agreement for $X/L < 0.3$. The two-layer method with $k_{wO} = 80$ cm/s also agrees with the measurements at $X/L > 0.5$. At the lower altitude (Figs. 13 and 15), the two-layer methods yield better agreement for $X/L > 0.2$

In the higher altitude cases (Figs. 12 and 14), the nonequilibrium axisymmetric viscous shock-layer methods with the temperature-dependent γ_O and γ_N yield good agreement at $X/L < 0.3$ and the nonequilibrium two-layer with $k_{wO} = 80$ cm/s and $k_{wN} = 24$ cm/s yields good agreement for $X/L < 0.5$. For the lower altitude case, this two-layer approach yields better agreement for $X/L > 0.2$ than the axisymmetric viscous shock-layer methods. The nonequilibrium two-layer method using temperature-dependent γ_O and γ_N results are about 30% higher than the measurements on the nose area for all cases presented here, but the agreement improves toward the middle of the vehicle and at lower altitude. It is apparent that

the two-layer approach predicts higher heat fluxes for given wall boundary conditions than do the viscous shock-layer approaches. This difference may be due in part to the VSL having a slightly higher level of dissociation as well as to differences in the flowfield modeling.

In comparing three-dimensional nonequilibrium calculations of Kim, Swaminathan, and Lewis[9] with other noncatalytic predictions, one sees that the heat flux does not decrease as rapidly down the vehicle as do the axisymmetric viscous shock-layer and two-layer calculations. This variation indicates a possible influence of geometry and crossflow that is more adequately accounted for in three-dimensional viscous shock-layer model. In Figs. 12 and 13, the three-dimensional viscous shock-layer results of Ref. 9 tend toward better agreement with the measurements than the other calculations aft of $X/L = 0.6$. This three-dimensional approach should be further investigated with appropriate finite rate recombination coefficients.

The increase in measured heat flux above the calculations of the aft half of the vehicle and especially for STS-5 may also have other explanations. The increase could be due to increasing recombination rates, but that would be inconsistent with the measurements on the forward part of the vehicle unless the aft is contaminated with a catalytic material. This contamination is possible because the adhesive used to bond the tiles to the structure contains various metal oxides, particularly iron oxide, which is known to be highly catalytic

The two-layer methods have been used to calibrate faster and more flexible codes to provide heat fluxes and other properties over a wider range of conditions than those for which the two-layer methods were applied. The nonequilibrium results of Stewart, Rakich, and Lanfranco[3] have been used by Rakich, Stewart, and Lanfranco[5] and Scott and Derry.[6] One of the weaknesses of these applications is the inability to account properly for variations in the flowfield chemical composition because parameters such as angle of attack, freestream density, and velocity differ from the few cases available in the three-dimensional Euler solutions. The axisymmetric shock-layer codes have the advantage of greater flexibility in running cases because of their fast computation time. Gupta et al.[16] investigated the influence of small variations in the angle of attack on the nonequilibrium heating and found the influence on heat flux to be small. A larger percentage variation was observed for lower velocities. This result may be due to greater temperature sensitivity of the level of oxygen dissociation at lower temperatures occurring in the lower-altitude case. Small changes in the component of velocity normal to the shock wave associated with the change in the angle of attack result in temperature changes in a range in which the oxygen dissociation is very sensitive. However, since the general sensitivity of absolute heat flux to angle of attack is small, the approximations made in Refs. 5 and 6 should not significantly degrade the accuracy.

The disadvantage of the axisymmetric viscous shock-layer methods is that they are capable of handling only bodies of revolution and they rely on angle-of-attack simulation via changing the body profile. Cross flow or transverse body curvature is therefore quite limited. Fortunately, for the present work, this has not been a strong limitation, but it may explain why there is disagreement with measurements on the aft of the vehicle.

The three-dimensional viscous shock-layer approach does away with those approximations, but has the disadvantage of requiring a shock shape as input (as do the axisymmetric viscous shock-layer solutions). The three-dimensional version has only recently been developed and will require further work to compare with measurements before its adequacy will be completely known.

The three-dimensional inviscid solution method coupled with the boundary-layer solutions requires a great deal of computer time to obtain the inviscid flowfield and also requires assumptions about how far to go into the inviscid flow from the body to obtain the boundary-layer edge conditions. Choosing the boundary-layer edge too far into the lower entropy flowfield will result in heating predictions that are too high. This may be the reason that the two-layer methods predicted higher results than did the axisymmetric viscous shock-layer method for the noncatalytic case at $X/L > 0.02$ and for the fully catalytic case at $0.02 < X/L < 0.2$. The noncatalytic case is more sensitive to the dissociation level, which is higher in the flow that has undergone a stronger shock.

Although energy-transfer catalytic recombination coefficients for nitrogen and oxygen recombination on HRSI have been measured in arcjet facilities,[7] the temperature range for γ_O did not extend to temperatures low enough to cover the range encountered in the Orbiter flights. There have been several attempts to infer catalytic recombination coefficients from the flight measurements, but this inference is difficult for several reasons. First, the flowfield is composed of oxygen and nitrogen atoms in varying amounts according to the vehicle trajectory and location on the vehicle. If one chooses a lower velocity condition where very little nitrogen is dissociated, then it may be possible to infer k_{wO}. However, we have seen a flight-to-flight measurement uncertainty of at least 15% and a prediction-to-prediction variation of the same magnitude. Heating uncertainties of this magnitude result in k_w uncertainties on the order of a factor of five.[16] Therefore, such a procedure should be used with great caution. This illustrates the need for careful ground experiments or great fidelity in the flight heat-flux calculations to obtain accurate recombination coefficients. The ground measurements of Scott,[7,17] as any ground measurements, require either precise heat flux calculations or a reliable reference surface with which to compare the heating or both. Even then, accurate results are difficult. Fortunately, only moderately accurate recombination coefficients are required to calculate reasonably accurate heating rates.

Ascertaining the nitrogen recombination coefficients from flight measurements is almost impossible without a knowledge of the coefficients for oxygen, because the oxygen atom is always an important species in the flow whenever there is any dissociated nitrogen. If the flowfield and k_{wO} were known accurately as a function of T_w, then it might be possible to infer k_{wN}.

Heating to Highly Catalytic Tiles

Attention is now turned to the results of the NASA Ames Research Center's catalytic surface effects Orbiter experiment.[3,5] Not only did this very significant experiment demonstrate the noncatalytic nature of the RCG-coated tiles, it also may give some clues as to the variation of dissociation in the boundary layer and the wall recombination rates. On STS-2, two tiles were painted with a highly catalytic material: iron-cobalt-chromia spinel (C742) developed by Stewart et al.[3] at Ames. The predicted and measured heat fluxes in the vicinity of the two C742-coated tiles on the bottom centerline of the Orbiter during STS-2 re-entry are given in Figs. 16 and 17, respectively. The measurements were obtained at 475 s after 122 km altitude was reached. At the forward location near the nose, the two-layer calculation using the method and recombination rates of Rakich et al.[5] yields the best agreement with the measurements. This should be the case because the recombination coefficients were inferred from the measurements at this location and approximate entry time. Also shown is the same calculation using the recombination coefficients obtained from arcjet measurements.[7,17] As seen in Fig. 16 (the forward location), the increase in heat flux on the C742-coated tile is larger for the Rakich recombination rates than for the recombination rates of Refs. 7 and 17, even though the latter rates for C742 are larger. The reason for this behavior is that, because of the higher RCG recombination rates of Ref. 7, the boundary layer is depleted of atomic nitrogen and oxygen so that when the flow reaches the C742-coated tile, there is not

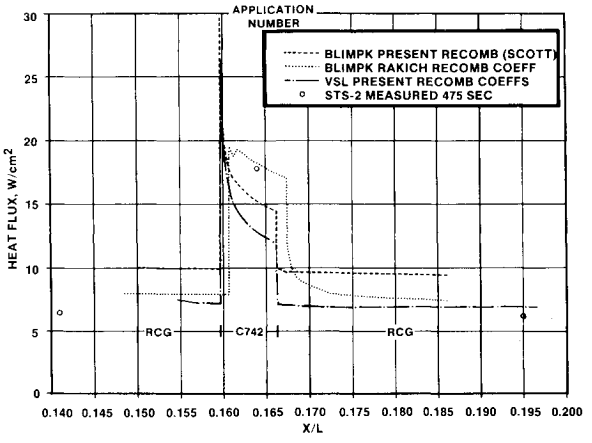

Fig. 16 Heat fluxes on C742-coated tile at $X/L = 0.163$, STS-2, $t = 475$ s ($V_{INF} = 7.16$ km/s, ALT = 74.7 km).

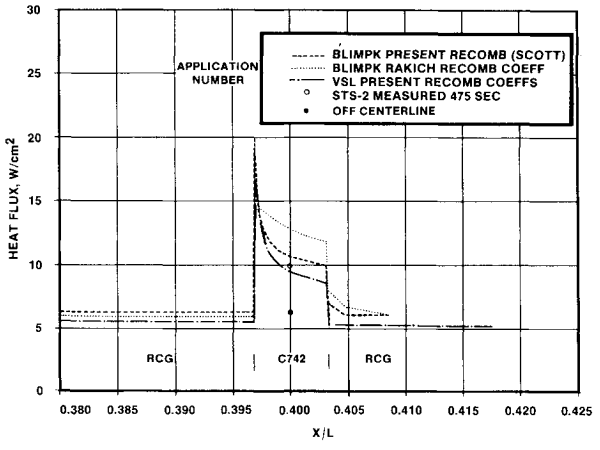

Fig. 17 Heat fluxes on C742-coated tile at $X/L = 0.40$, STS-2, $t = 475$ s ($V_{INF} = 7.16$ km/s, ALT = 77.7 km).

much chemical energy available for transfer to the highly catalytic tile. A similar behavior is seen at $X/L = 0.4$ in Fig. 17. Since the recombination rates of Refs. 7 and 17 increase with temperature, the upstream edge of the C742-coated tile is exposed to a high heat flux that decreases rapidly because of the depletion of atoms in the boundary layer—a condition leading to further reduction in the recombination rate along the tile as the temperature decreases.

The agreement in heat flux between the axisymmetric viscous shock-layer and boundary-layer methods is not very good on the C742-coated tiles. The heat flux calculated by the VSL method drops much more rapidly, possibly because of the more rapid depletion of atoms in the boundary layer than the boundary-layer method predicts. There also seems to be some sensitivity of the heat flux distribution along the tile to the streamwise nodal spacing used in the calculation.

On STS-5, the heating did not increase above the noncoated tiles as much as on STS-2 and STS-3. This result is consistent with the noncoated tiles having an increased catalycity that would deplete more of the boundary-layer atoms than on the earlier flights; therefore, the recombination heating on the overcoated tiles would be less.

For the STS-5 flight, an additional strip of tiles (1.5 m long and 15 cm wide) forward of, and including the $X/L = 0.4$ centerline location, was coated with the C742 catalytic coating. This was done to investigate the possibility of the boundary layer relaxing to a condition similar to a completely catalytic vehicle. The heat flux at $X/L = 0.4$ aft of the coated strip was lower than an isolated tile. (Compare STS-2, STS-3, and STS-5 in Figs. 1-3.) These results do indicate that there is relaxation toward the uniform surface heating rate. However,

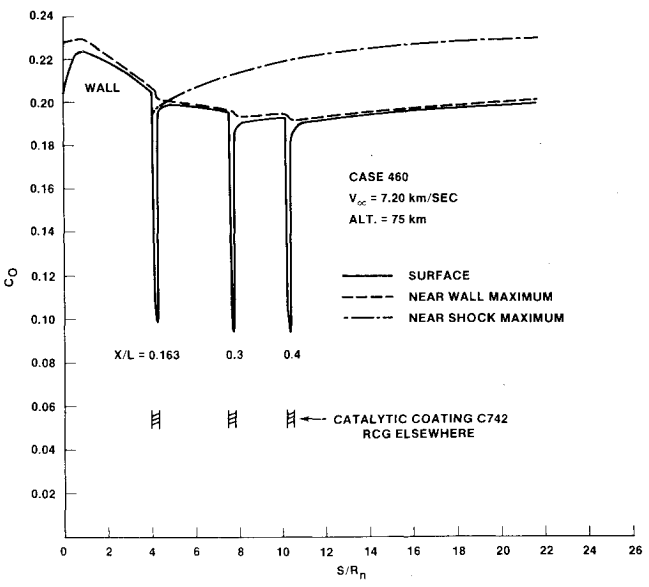

Fig. 18 Oxygen atom concentrations on surface and in shock-layer calculated by viscous shock-layer method.

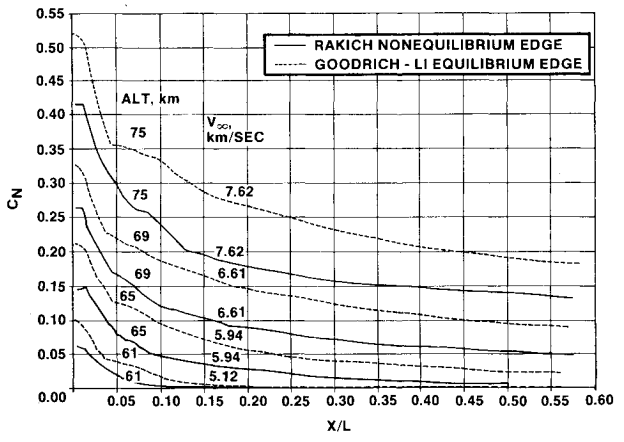

Fig. 19 Nitrogen atom mass fraction on centerline of Orbiter at boundary-layer edge.

Ref. 3 and unpublished calculations by the author have shown that this relaxation is significant, but is not complete over a strip only 1.5 m long. Therefore, one could not assume that the heat flux at $X/L = 0.4$ represents the heating to a uniformly coated, fully catalytic vehicle.

Figure 18 gives the oxygen atom concentration at the surface and the peak oxygen concentrations near the surface and near the shock wave using the Miner and Lewis code[13] for case 460. It is seen that the atom concentration decreases sharply by about a factor of one-half at the locations having the high catalycity, e.g., where the tiles have the C742 coating. The disturbance in atom concentration is also seen in the peak atom concentration near the surface, a few millimeters from the wall. There is no discernible influence due to the overcoated tiles far from the wall at a concentration maximum near the shock wave. This is as expected.

Nonequilibrium Atom Concentrations

In most of the flight regime associated with high heat flux, the oxygen near the surface is fully dissociated. (See Refs. 1 and 8.) However, the nitrogen is substantially less than fully dissociated. The Rakich calculations for inviscid reacting flow boundary-layer edge conditions and the Goodrich corresponding equilibrium edge nitrogen concentration are presented in Fig. 19. At the higher velocity and altitude cases, there is substantial nitrogen dissociation even at $X/L \sim 0.5$. At lower

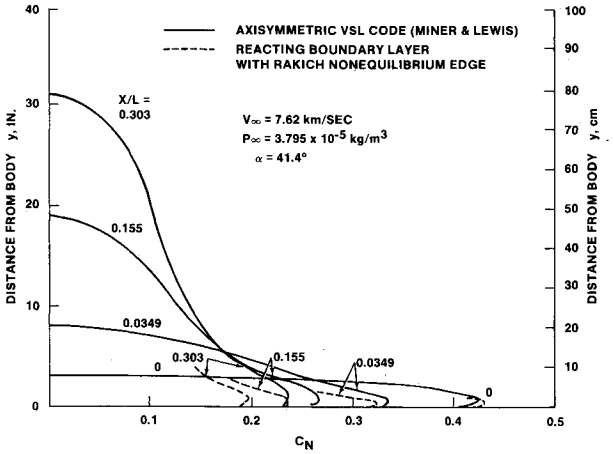

Fig. 20 Nitrogen atom mass fraction as a function of distance from body: comparison of axisymmetric viscous shock-layer method and reacting boundary layer with nonequilibrium edge.

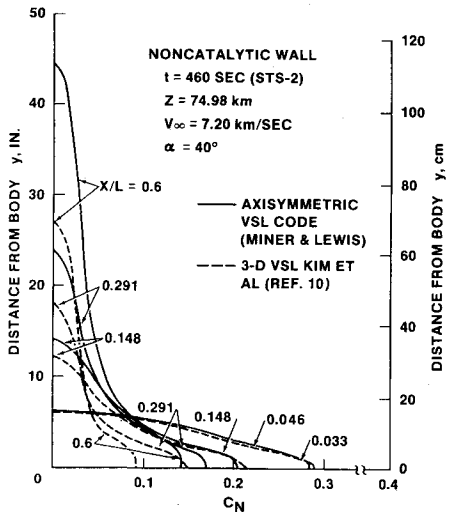

Fig. 21 Nitrogen atom mass fraction as a function of distance from body: comparison of axisymmetric viscous shock-layer method with three-dimensional viscous shock-layer results for noncatalytic wall.

velocities, the nitrogen is substantially dissociated on the nose of the vehicle, but very little is dissociated at the middle. At velocities as low as 5 km/s, there is very little nitrogen dissociation even on the nose. Substantial nitrogen dissociation is taken to mean that the nitrogen dissociation energy $C_N h_{DN}$ is comparable to or larger than that of oxygen, $C_O h_{DO}$. The enthalpy of dissociation of nitrogen h_{DN} is about twice that of oxygen h_{DO}. It can be seen from Fig. 19 that the equilibrium prediction of nitrogen atom concentration C_N is always larger than the corresponding nonequilibrium prediction. This result implies that the dissociation reaction never goes to completion in the flow time available.

It appears that nitrogen nonequilibrium exists throughout the entry regime where nitrogen dissocation is significant. It is seen that the nonequilibrium nitrogen concentration approaches the equilibrium concentration only for very small concentrations.

It was pointed out[1] that the component of heat flux resulting from diffusion is influenced more by the normal shock flow near the surface than by the so-called boundary-layer edge atom concentration. This fact is graphically illustrated in Fig. 20, where it can be seen that the nitrogen atom concentration next to the noncatalytic wall is higher than the "edge" concentration. The concentration C_N decreases as the flow moves down the surface, demonstrating nitrogen gas-phase recombination near the surface. The concentration at

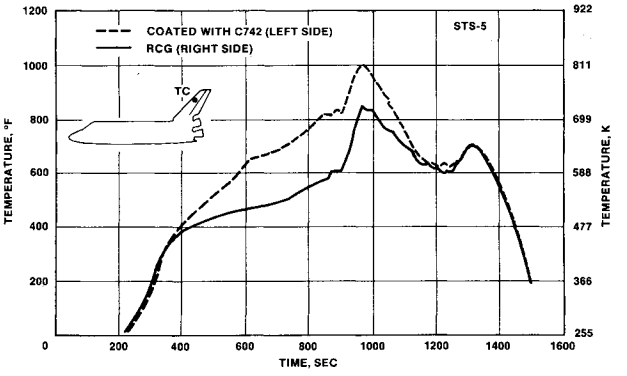

Fig. 22 Temperatures on vertical stabilizer tiles with and without catalytic coating.

the boundary-layer edge is also decreasing, because of lower dissociation in the flow from a weaker shock wave. It appears in Fig. 20 that the nonequilibrium viscous shock-layer calculation results in a somewhat larger amount of nitrogen dissociation than Rakich's inviscid results away from the stagnation point. This may be part of the reason why the noncatalytic viscous shock-layer heat flux results are lower than the boundary-layer results seen in Figs. 6 and 7. A similar difference in heating is seen in Fig. 9, where the three-dimensional VSL heating results are higher than the axisymmetric results. Lower heating to a noncatalytic surface is expected when more of the energy is tied up in dissociation as seen in Fig. 21.

The thicker shock layer and higher C_N seen for the axisymmetric VSL code may be a result of the assumed geometry, i.e., the hyperboloid of revolution as opposed to the actual three-dimensional geometry of the Shuttle Orbiter.

Leeward Side Nonequilibrium

This paper has been primarily concerned with the nonequilibrium flow on the windward side of the Orbiter because it is there that the prediction techniques have been developed to date. As three-dimensional computational capability advances, the leeward and wake regions during re-entry will be of increased interest. As an adjunct to the Ames catalytic surface effects experiment, one tile on the vertical stabilizer was coated with C742 for flight STS-5. The tile was instrumented with a surface thermocouple, and, likewise, an uncoated tile on the opposite side of the stabilizer was instrumented with a surface thermocouple. The temperature history during re-entry is presented in Fig. 22. It is seen that the temperature of the C742-coated tile was as much as 111 K (200°F) hotter than the basic (RCG) tile. This difference in temperature implies about a factor of two difference in heat flux that results from a dissociated leeward side flowfield and nonequilibrium in the vicinity of the vertical stabilizer. Existence of nonequilibrium is not surprising, since the recombination reaction rate in the gas phase should be very small in the low-pressure and low-temperature expanded flow around the leeward side of the vehicle. It is presumed that the nonequilibrium dissociation persists far into the wake of the vehicle. This theory is evidenced by the afterglow trail of a re-entry body such as a meteor and has been observed during Orbiter re-entry.

Conclusions

This paper has attempted to evaluate the current state-of-the-art nonequilibrium flow tools applied to the Space Shuttle. From this discussion, the importance of nonequilibrium phenomena to the Space Shuttle re-entry heating has been assessed. Since the inception of the design of the Space Shuttle more than 14 years ago, there have been developments in heat flux prediction methodologies. Initially, nonequilibrium and surface catalysis effects were ignored, which led to a design that exceeded the requirements in many areas, but also

resulted in an added margin of safety in other areas that proved beneficial.

It was found that the normalized heat fluxes measured on the windward centerline of the Orbiter tended to increase from flight to flight. Roughly, a 20% change was noted from STS-2 to STS-5 at most of the thermocouple locations, indicating changes in surface properties such as emittance or catalycity.

The nonequilibrium heat flux methods that have been developed and the catalycity measurements obtained over the past decade have improved the prediction capability from a 20-100% overprediction for an assumed fully catalytic surface material to an accuracy of about 10-30% for nearly non-catalytic materials, e.g., the RCG coating on HRSI. These methods are the two-layer inviscid three-dimensional reacting flowfield coupled with the reacting boundary layer and the reacting viscous shock-layer solutions. The application of these methods may result in more appropriate reliance on wind tunnel measurements, which cannot simulate the high-enthalpy reacting flow associated with orbital re-entry. Indeed, calculations are necessary for such a simulation.

As the comparisons of the predictions with the measurements from the Space Shuttle flight tests have shown, we are now in a position of refining the prediction techniques and determining those phenomena that will be of significance for the design of future re-entry vehicles such as an aeroassisted orbital transfer vehicle (AOTV). Although nonequilibrium calculation techniques using finite-rate catalycity wall boundary conditions have significantly improved the prediction capability, none of the methods yields good agreement uniformly for all locations and freestream conditions. This points to the need for further refinement in these methods. The three-dimensional viscous approaches in particular should be pursued, since the trends of the heating profiles tend to be better than for the other methods.

Nitrogen recombination is seen to be a very important phenomenon on the nose and elsewhere at the higher velocities. This means that the accuracy of the nitrogen recombination coefficients is important to the heat flux predictions in those areas. Since the AOTV enters the atmosphere at higher speeds and remains at higher altitudes where nonequilibrium flow dominates, the nitrogen gas and surface reactions will be especially important. Since most of the Shuttle data were obtained in regimes where oxygen dissociation predominated, further flight and ground investigations of nitrogen should be pursued.

Acknowledgments

The author expresses his thanks to Dr. W. D. Goodrich for furnishing equilibrium edge conditions for boundary-layer calculations. The author is indebted to John V. Rakich for furnishing nonequilibrium edge conditions. His recent untimely death was a source of deep regret to his friends in the aerospace community.

References

[1]Scott, C. E., "Space Shuttle Laminar Heating with Finite-Rate Catalytic Recombination," *Progress in Astronautics and Aeronautics: Thermophysics,* Vol. 82, edited by T. E. Horton, AIAA, New York, 1982, pp. 273-289.

[2]Rakich, J. V. and Lanfranco, M. J., "Numerical Computation of Space Shuttle Laminar Heating and Surface Streamlines," *Journal of Spacecraft and Rockets,* Vol. 14, May 1977, pp. 265-272.

[3]Stewart, D. A., Rakich, J. V., and Lanfranco, M. J., "Catalytic Surface Effects Experiment on the Space Shuttle," *Progress in Astronautics and Aeronautics: Thermophysics of Atmospheric Entry,* Vol. 82, edited by T. E. Horton, AIAA, New York, 1982, pp. 248-272.

[4]Stewart, D. A., Rakich, J. V., and Lanfranco, M. J., "Catalytic Surface Effects of Space Shuttle Thermal Protection System During Earth Entry of Flights STS-2 through STS-5," Paper presented at Langley Conference on Shuttle Performance: Lessons Learned, Hampton, Va., March 1983.

[5]Rakich, J. V., Stewart, D. A., and Lanfranco, M. J., "Results of a Flight Environment on the Catalytic Efficiency of the Space Shuttle Heat Shield," AIAA Paper 82-0944, June 1982.

[6]Scott, C. D. and Derry, S. M., "Catalytic Recombination and the Space Shuttle Heating," AIAA Paper 82-0841, June 1982.

[7]Scott, C. D., "Catalytic Recombination of Oxygen and Nitrogen in High Temperature Reusable Surface Insulation," *Progress in Astronautics and Aeronautics: Aerothermodynamics and Planetary Entry,* Vol. 77, edited by A. L. Crosbie, AIAA, New York, 1981 pp. 192-212.

[8]Shinn, J. L., Moss, J. N., and Simmonds, A. L., "Viscous-Shock-Layer Heating Analysis for the Shuttle Windward Plane with Surface Finite Catalytic Recombination Rates," AIAA Paper 82-0842, June 1982.

[9]Kim, M. D., Swaminathan, S., and Lewis, C. H., "Three-Dimensional Nonequilibrium Flows Shock Layer Flows Over the Space Shuttle Orbiter," *Journal of the Spacecraft and Rockets,* Vol. 21, Jan.-Feb. 1984, pp. 29-35.

[10]Kim, M. D., Swaminathan, S., and Lewis, C. H., "Viscous Shock-Layer Predictions of Three-Dimensional Nonequilibrium Flows Past the Space Shuttle at High Angle of Attack," Paper presented at the Langley Conference of Shuttle Performance: Lessons Learned, Hampton, Va., March, 1983.

[11]Harthun, M. H., Blumer, C. B., and Miller, B. A., "Orbiter Windward Surface Entry Heating-Post-Orbital Flight Test Program Update," Paper presented at the Langley Conference on Shuttle Performance: Lessons Learned, Hampton, Va., March, 1933.

[12]Moss, J. N., "Reacting Viscous-Shock-Layer Solutions with Multicomponent Diffusion and Mass Injection," NASA TR R-411, June 1974.

[13]Miner, E. W. and Lewis, C. H., "Hypersonic Ionizing Air Viscous Shock-Layer Flows Over Nonanalytical Blunt Bodies," NASA CR-2550, May 1975.

[14]Goodrich, W. D., Li, C. P., Houston, C. K., Chin, P. B., and Olmedo, L., "Numerical Computations of Orbiter Flowfields and Laminar Heating Rates," *Journal of Spacecraft and Rockets,* Vol. 14, May 1977, pp. 257-264.

[15]Zoby, E. V., "Analysis of STS-2 Experimental Heating Rates and Transition Data," AIAA Paper 82-0822, June 1982.

[16]Gupta, R. N., Moss, J. N., Simmonds, A. L., Shinn, J. L., and Zoby, E. V., "Space Shuttle Heating Analysis with Variation in Angle-of-Attack and Surface Condition," AIAA Paper 83-0486, Jan. 1983.

[17]Scott, C. D., "Catalytic Recombination of Nitrogen and Oxygen on Iron-Cobalt-Chromia Spinel," AIAA Paper 83-0585, Jan. 1983.

[18]Bartlett, E. P. and Kendall, R. M., "'An Analysis of the Coupled Chemically Reacting Boundary Layer and Charring Ablator, Pt. III: Nonsimilar Solution of the Multicomponent Laminar Boundary Layer by an Integral Matrix Method," NASA CR-1062, June 1968.

[19]Tong, H., Buckingham, A. D., and Morse, H. L., "Nonequilibrium Chemistry Boundary Layer Integral Matrix Procedure," NASA CR-134039, July 1973.

[20]Williams, S. D. and Curry, D. M., "An Analytical and Experimental Study for Surface Heat Flux Determination," *Journal of Spacecraft and Rockets,* Vol. 14, Oct. 1977, pp. 632-637.

[21]Bradley, P. F., Siemers, P. M. III, and Weilmuenster, K. J., "An Evaluation of Space Shuttle Orbiter Forward Fuselage Surface Pressures: Comparison with Wind Tunnel and Theoretical Predictions," AIAA Paper 83-0119, Jan. 1983.

[22]Blottner, F. G., "Nonequilibrium Laminar Boundary-Layer Flow of Ionized Air," General Electric, Valley Forge, Pa., R64SD56, Nov. 1964.

[23]Gupta, R. N., Moss, J. N., Simmonds, A. L., Shinn, J. L., and Zoby, E. V., "Space Shuttle Heating Analysis with Variation in Angle of Attack and Surface Conditions," AIAA Paper 83-0486, Jan. 1983.

[24]Zoby, E. V., Gupta, R. N., and Simmonds, A. L., "Temperature-Dependent Reaction-Rate Expression for Oxygen Recombination of Shuttle Entry Conditions," AIAA Paper 84-0224, Jan. 1984.